We are IntechOpen, the world's leading publisher of Open Access books Built by scientists, for scientists

4,800
Open access books available

122,000
International authors and editors

135M
Downloads

Our authors are among the

154
Countries delivered to

TOP 1%
most cited scientists

12.2%
Contributors from top 500 universities

CLARIVATE ANALYTICS BOOK CITATION INDEX INDEXED

WEB OF SCIENCE™

Selection of our books indexed in the Book Citation Index in Web of Science™ Core Collection (BKCI)

Interested in publishing with us?
Contact book.department@intechopen.com

Numbers displayed above are based on latest data collected.
For more information visit www.intechopen.com

14

Introduction to Doubly-Fed Induction Generator for Wind Power Applications

Dr John Fletcher and Jin Yang
University of Strathclyde, Glasgow
United Kingdom

1. Introduction

This chapter introduces the operation and control of a Doubly-fed Induction Generator (DFIG) system. The DFIG is currently the system of choice for multi-MW wind turbines. The aerodynamic system must be capable of operating over a wide wind speed range in order to achieve optimum aerodynamic efficiency by tracking the optimum tip-speed ratio. Therefore, the generator's rotor must be able to operate at a variable rotational speed. The DFIG system therefore operates in both sub- and super-synchronous modes with a rotor speed range around the synchronous speed. The stator circuit is directly connected to the grid while the rotor winding is connected via slip-rings to a three-phase converter. For variable-speed systems where the speed range requirements are small, for example ±30% of synchronous speed, the DFIG offers adequate performance and is sufficient for the speed range required to exploit typical wind resources.
An AC-DC-AC converter is included in the induction generator rotor circuit. The power electronic converters need only be rated to handle a fraction of the total power – the rotor power – typically about 30% nominal generator power. Therefore, the losses in the power electronic converter can be reduced, compared to a system where the converter has to handle the entire power, and the system cost is lower due to the partially-rated power electronics. This chapter will introduce the basic features and normal operation of DFIG systems for wind power applications basing the description on the standard induction generator. Different aspects that will be described include their variable-speed feature, power converters and their associated control systems, and application issues.

2. Steady-state operation of the Doubly-Fed Induction Generator (DFIG)

The DFIG is an induction machine with a wound rotor where the rotor and stator are both connected to electrical sources, hence the term 'doubly-fed'. The rotor has three phase windings which are energised with three-phase currents. These rotor currents establish the rotor magnetic field. The rotor magnetic field interacts with the stator magnetic field to develop torque. The magnitude of the torque depends on the strength of the two fields (the stator field and the rotor field) and the angular displacement between the two fields. Mathematically, the torque is the vector product of the stator and rotor fields. Conceptually, the torque is developed by magnetic attraction between magnet poles of opposite polarity where, in this case, each of the rotor and stator magnetic fields establish a pair of magnet

poles, Fig 1. Clearly, optimum torque is developed when the two vectors are normal to each other. If the stator winding is fed from a 3-phase balanced source the stator flux will have a constant magnitude and will rotate at the synchronous speed.

We will use the per-phase equivalent circuit of the induction machine to lay the foundations for the discussion of torque control in the DFIG. The equivalent circuit of the induction machine is shown in Fig.2.

The stator side has two 'parasitic' components, R_s and L_s, which represent the resistance of the stator phase winding and the leakage inductance of the phase winding respectively. The leakage inductance models all the flux generated by current in the stator windings that does not cross the air-gap of the machine, it is therefore not useful for the production of torque. The stator resistance is a natural consequence of the windings being fabricated from materials that are good conductors but nonetheless have finite conductance (hence resistance).

The magnetising branch, L_m, models the generation of useful flux in the machine – flux that crosses the air-gap either from stator to rotor or vice-versa.

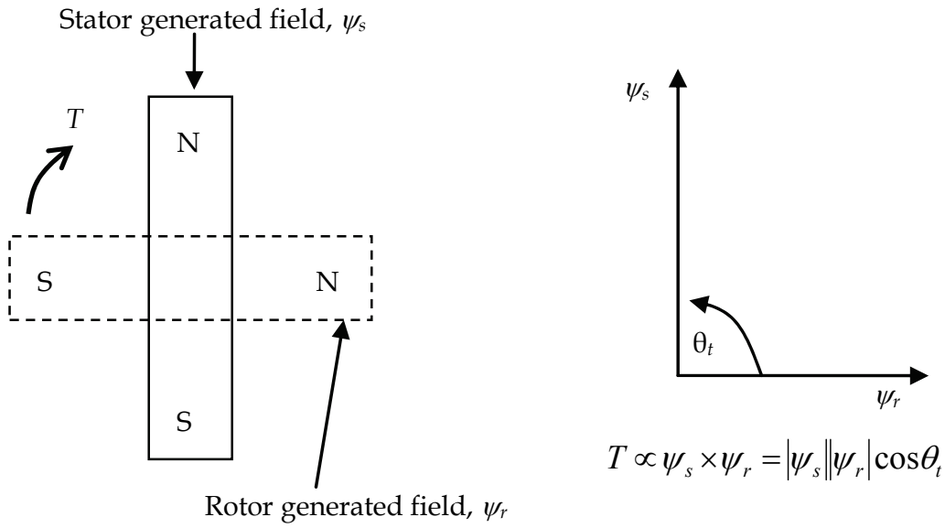

Fig. 1. Magnetic pole system generated by currents in the stator and rotor windings. The stator and the rotor field generate a torque that tends to try and align poles of opposite polarity. In this case, of rotor experiences a clockwise torque.

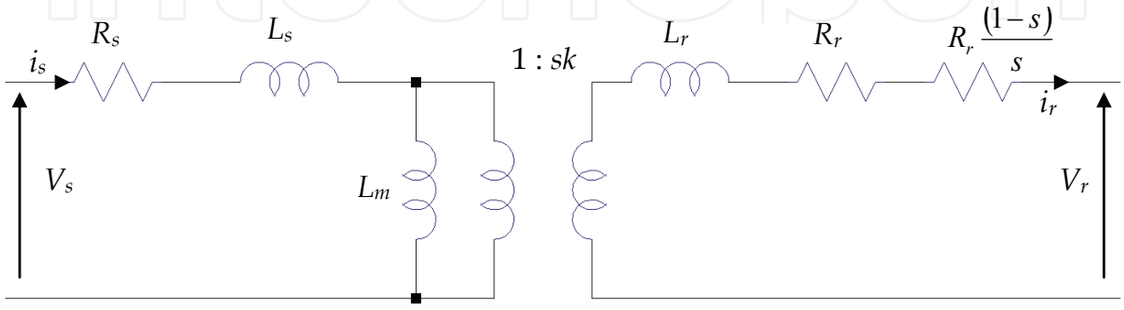

Fig. 2. Per-phase equivalent circuit of an induction machine.

Like the stator circuit, the rotor circuit also has two parasitic elements. The rotor leakage reactance, L_r, and the rotor resistance R_r. In addition, the rotor circuit models the generated mechanical power by including an additional rotor resistance component, $R_r(1–s)/s$. Note that the rotor and stator circuits are linked via a transformer whose turns ratio depends on the actual turns ratio between the stator and rotor (1:k), and also the slip, s, of the machine.
In an induction machine the slip is defined as

$$s = \frac{n_s - n_r}{n_s} \tag{1}$$

where n_s and n_r are the synchronous speed and the mechanical speed of the rotor respectively. The synchronous speed is given by

$$n_s = \frac{60 f_e}{p} \text{ rpm} \tag{2}$$

where p = number of pole pairs and f_e is the electrical frequency of the applied stator voltage.
We will first consider the operation of the machine as a standard induction motor. If the rotor circuit is left open circuit and the rotor locked (standstill), when stator excitation is applied, a voltage will be generated at the output terminals of the rotor circuit, V_r. The frequency of this output will be at the applied stator frequency as slip in this case is 1. If the rotor is turned progressively faster and faster in the sub-synchronous mode, the frequency at the output terminals of the rotor will decrease as the rotor accelerates towards the synchronous speed. At synchronous speed the rotor frequency will be zero. As the rotor accelerates beyond synchronous speed (the super-synchronous mode) the frequency of the rotor voltage begins to increase again, but has the opposite phase sequence to the sub-synchronous mode. Hence, the frequency of the rotor voltage is

$$f_r = sf_e \tag{3}$$

No rotor currents can flow with the rotor open circuit, hence there is no torque production as there is no rotor field ψ_r, Fig 1. If the rotor was short circuited externally, rotor currents can flow, and they will flow at the frequency given by (3). The rotor currents produce a rotor magnetic field, ψ_r, which rotates at the same mechanical speed as the stator field, ψ_s. The two fields interact to produce torque, Fig. 1.
It is important to recognise that the rotor magnetic field and the stator magnetic field both rotate at the synchronous speed. The rotor may be turning asynchronously, but the rotor field rotates at the same speed as the stator field.
The mechanical torque generated by the machine is found by calculating the power absorbed (or generated) by the rotor resistance component $R_r(1–s)/s$. This is shown to be

$$P_{mech} = 3|i_r|^2 \left(\frac{1-s}{s} \right) R_r \tag{4}$$

In an ideal induction machine, we can ignore the rotor and stator phase winding resistance and leakage inductance. The per-phase equivalent circuit then becomes simple, Fig. 3. The phasor diagram for the machine is shown. Note that the stator generated flux component is normal to the rotor current (hence rotor flux) phasor giving the optimum conditions for

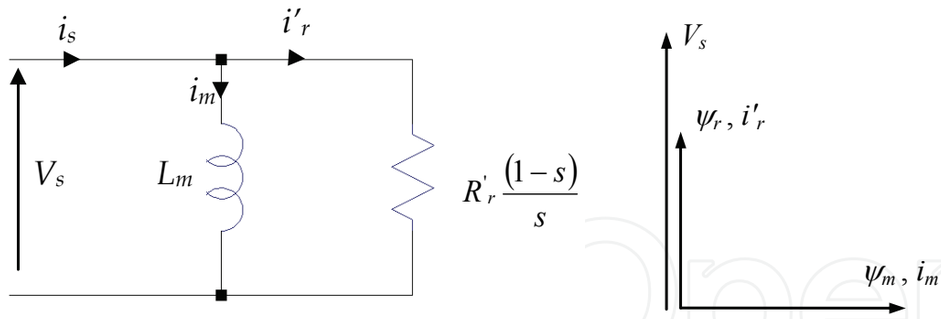

Fig. 3. Simplified equivalent circuit of the induction machine assuming low values of slip and negligible stator and rotor leakage reactance. Phasor diagram demonstrates optimal orientation of magnetising current and rotor current.

torque production (note this is true for low values of slip only). Using this simplified circuit diagram, the mechanical torque production is then:

$$T_{mech} = 3\left|i_r^{'}\right|^2 \left(\frac{1-s}{s}\right)\frac{R_r^{'}}{\omega_m} \tag{5}$$

$$\text{As } \omega_m = \frac{(1-s)\omega_m}{p} \text{ and } \psi_m = L_m i_m = \frac{V_s}{\omega_s} = \frac{\left|i_r^{'}\right| R_r^{'}}{s\omega_s} \tag{6}$$

Then

$$T_{mech} = 3\left|i_r^{'}\right|^2 \left(\frac{1-s}{s}\right)\frac{R_r^{'}}{\omega_m} = 3p\frac{\left|i_r^{'}\right| R_r^{'}}{s\omega_s}\left|i_r^{'}\right| = 3p\psi_m\left|i_r^{'}\right| \tag{7}$$

The key point in this development is to show that the developed torque is controlled by the combination of the stator generated flux, ψ_m, and the rotor current magnitude, i_r', if the two vectors are maintained in quadrature, Fig. 1. In the DFIG system, torque is controlled by calculating the physical position and magnitude of the stator generated flux (by monitoring the position and magnitude of the applied stator voltage which in this case is imposed by the grid voltage magnitude, frequency and phase) and regulating the rotor currents such that they are normal to the stator flux with a magnitude that will generate the desired torque.

The DFIG system therefore has to control the magnitude, frequency and phase of the applied rotor current. Most DFIG systems utilise closed-loop current control using a voltage-source inverter (VSI). At this stage, the voltage source inverter can be viewed as a three-phase voltage source whose magnitude and phase can be altered instantaneously – this will be illustrated in Section 2. Therefore, the VSI can be used to regulate the rotor current. In order to properly position the rotor current knowledge of the physical position of the rotor is required using a mechanical position sensor, for example. In such a way, the rotor current (hence flux) can be oriented optimally with respect to the stator flux to generate the desired torque.

3. Rotor power converters

This section will detail the AC-DC-AC converter used on the rotor which consists of two voltage-sourced converters, i.e., rotor-side converter (RSC) and grid-side converter (GSC),

which are connected "back-to-back." Between the two converters a dc-link capacitor is placed, as energy storage, in order to keep the voltage variations (or ripple) in the dc-link voltage small. With the rotor-side converter it is possible to control the torque or the speed of the DFIG and also the power factor at the stator terminals, while the main objective for the grid-side converter is to keep the dc-link voltage constant regardless of the magnitude and direction of the rotor power. The grid-side converter works at the grid frequency (leading or lagging in order to generate or absorb a controllable magnitude of reactive power). A transformer may be connected between the grid-side inverter or the stator, and the grid. The rotor-side converter works at different frequencies, depending on the wind speed.

The back-to-back arrangement of the converters provides a mechanism of converting the variable voltage, variable frequency output of the generator (as its speed changes) into a fixed frequency, fixed voltage output compliant with the grid. The DC link capacitance is an energy storage element that provides the energy buffer required between the generator and the grid.

The back-to-back inverter-converter arrangement

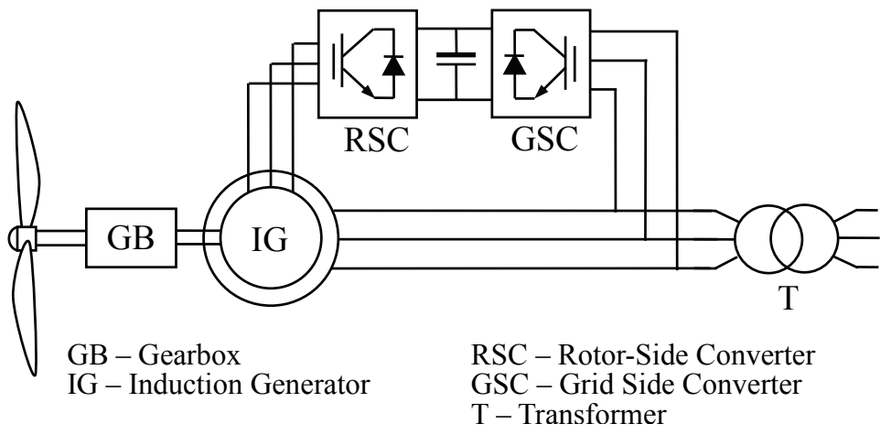

Fig. 4. Typical back-to-back arrangement of inverter and converter circuits to control power flow.

At the current state of development, most DFIG power electronics utilise a two-level six-switch converter, Fig. 4. Two-level refers to the number of voltage levels that can be produced at the output of each bridge leg of the converter. A two-level converter can typically output zero volts or V_{dc}, where V_{dc} is the voltage of the dc link. Fig. 4 shows two such converters connected in a back-to-back arrangement with a DC link between the two converters. The switching elements in higher power converters are likely to be Insulated-gate Bipolar Transistors (IGBTs). The six-switch converter can synthesise a three-phase output voltage which can be of arbitrary magnitude, frequency and phase, within the constraint that the peak line voltage is less than the DC link voltage. The converter is capable of changing the output voltage almost instantaneously – the limit is related to the switching frequency of the pulse-width modulated switching devices, and delays introduced by any filtering on the output (typical on the grid-side converter). The converter switches are switched ON and OFF with a fixed frequency but with a pulse-width that is varied in order to control the output voltage.

The voltage source inverter

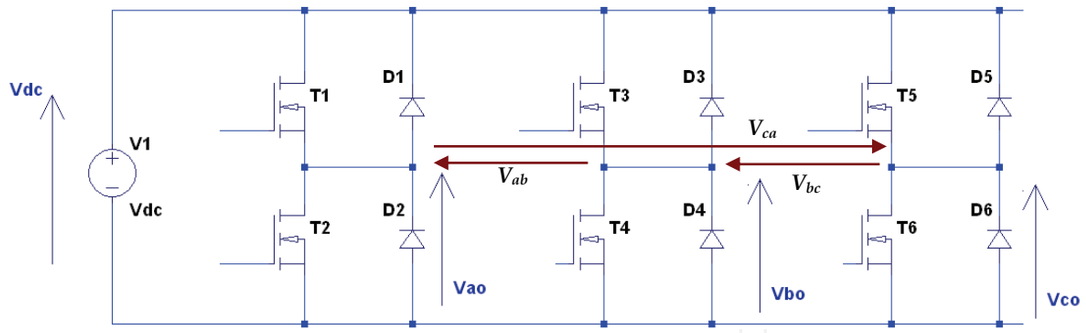

Fig. 5. Six-switch voltage source inverter circuit.

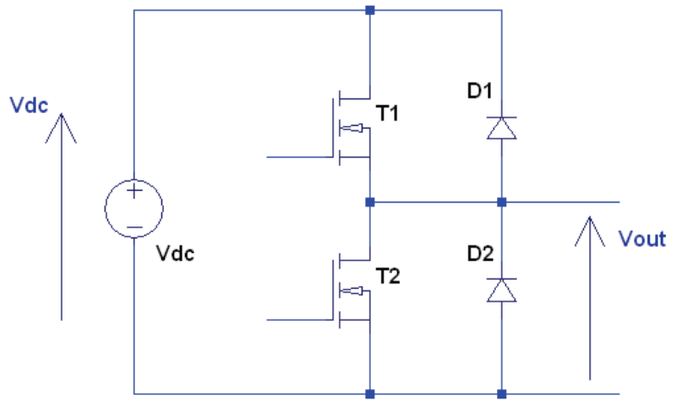

Fig. 6. One bridge leg of a voltage source inverter circuit.

Fig. 5 shows a six-switch inverter topology. It comprises three bridge legs in parallel. Fig. 6 shows one bridge leg. When switch T1 is ON, the output voltage, V_{out}, is V_{dc}. When switch T2 is ON, the output voltage is zero. (Note that both switches are not turned on at the same time). If the output is periodically switched between these two states, the output voltage, V_{out}, averaged over each switching period, can be controlled between zero volts and V_{dc}. The switching cycle is usually fixed, and the width of the pulse of V_{dc} adjusted in order to change the output voltage. Fig. 7 shows an example of a pulse-width modulated signal and indicates how the width of the pulse can be varied by comparing the modulating waveform with the carrier waveform – this is now mainly performed digitally but is also easy to implement in analogue electronics. The average output voltage, at the terminals of the bridge leg, V_{out}, is given by

$$V_{out} = V_{dc} \frac{t_{1,on}}{T_{sw}} \tag{8}$$

Where T_{sw} is the switching period, and $t_{1,on}$ is the on time of the switch T1. We define the duty cycle, or modulation index, m as

$$m = \frac{t_{1,on}}{T_{sw}} \tag{9}$$

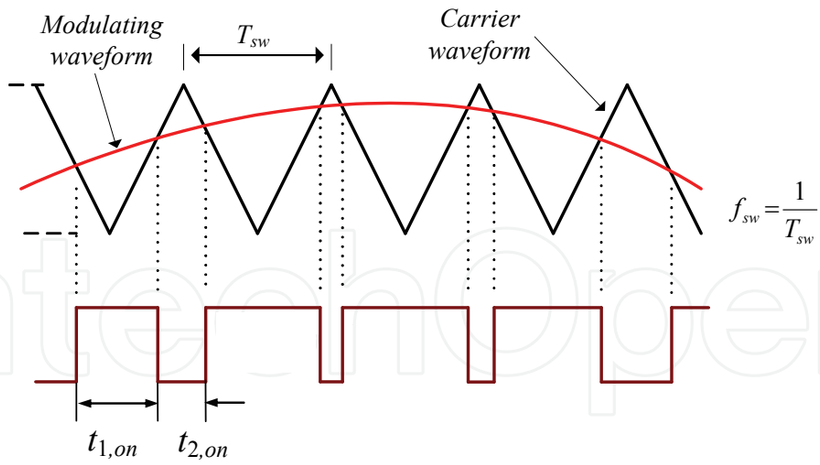

Fig. 7. Example of carrier-based pulse-width modulated signal generation.

Hence

$$V_{out} = m V_{dc} \tag{10}$$

where m must be between 0 (T2 on continuously) and 1 (T1 on continuously). The modulation index, m, can be varied in time, therefore any desired voltage and frequency can be generated at the output terminals (within the bounds fixed by the switching frequency and V_{dc}).

In the three-phase converter shown in Fig 5, there are three phase legs, hence three modulation indices, m_a, m_b and m_c. The voltages between the mid-point of each phase leg and the 0V node of the dc link are

$$\begin{cases} V_{ao} = m_a V_{dc} \\ V_{bo} = m_b V_{dc} \\ V_{co} = m_c V_{dc} \end{cases} \tag{11}$$

Now if each modulation index varies sinusoidally according to

$$\begin{cases} m_a = \frac{1}{2} + m\sin(\omega t) \\ m_b = \frac{1}{2} + m\sin\left(\omega t - 2\pi/3\right) \\ m_c = \frac{1}{2} + m\sin\left(\omega t + 2\pi/3\right) \end{cases} \tag{12}$$

Then the resultant output line voltages will take the from

$$\begin{cases} V_{ab} = V_{ao} - V_{bo} = \sqrt{3} m V_{dc} \sin\left(\omega t - \frac{\pi}{6}\right) \\ V_{bc} = V_{bo} - V_{co} = \sqrt{3} m V_{dc} \sin\left(\omega t - \frac{5\pi}{6}\right) \\ V_{ca} = V_{co} - V_{ao} = \sqrt{3} m V_{dc} \sin\left(\omega t + \frac{\pi}{2}\right) \end{cases} \tag{13}$$

These are three-phase, balanced output line voltages, whose magnitude is controlled by m and whose output frequency and phase can be regulated by the frequency and phase of the modulating waveform. The modulating waveforms can be manipulated digitally using high-performance microcontrollers or digital signal processors.

The VSI is capable of generating any voltage with arbitrary frequency and phase (within the limits of dc link voltage and switching frequency). Therefore, the VSI can be viewed and modelled as an ideal controllable voltage source whose bandwidth is usually much higher than the required excitation frequency required by the system. For example, Fig. 9 shows a single line diagram of a grid-connected inverter. In this case the inverter is simply modelled as an ideal voltage source that is generating a balanced set of three-phase voltages whose magnitude and phase can be controlled relative to the grid voltage. This provides the capability to control the flow of real and reactive power to the grid as will be discussed later. Note that synchronisation to the grid frequency is assumed.

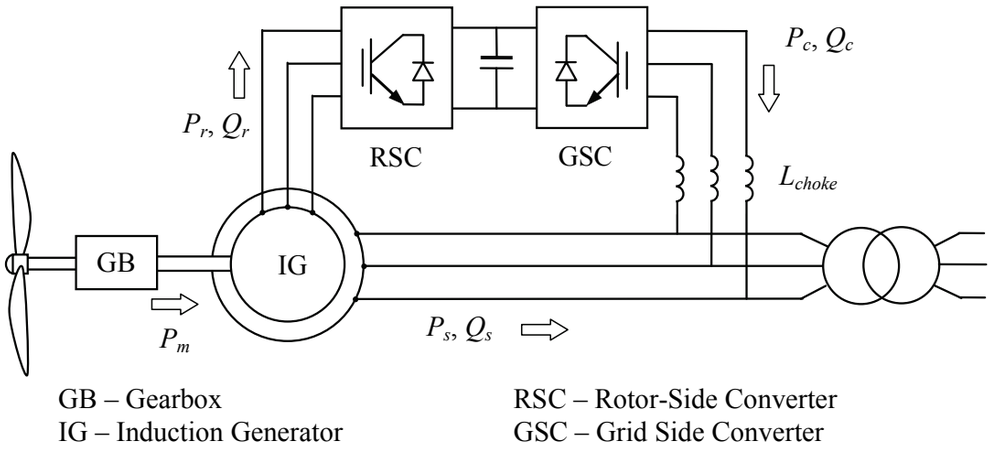

Fig. 8. Doubly-fed induction generation system power flows.

In steady-state at fixed turbine speed for a lossless DFIG system, the mechanical power from the wind turbine applied to the shaft is $P_m = P_s + P_r$. It follows that:

$$P_r = P_m - P_s = T_m\omega_r - T_{em}\omega_s = -T_m\left(\frac{\omega_s - \omega_r}{\omega_s}\right)\omega_s = -sT_m\omega_s = -sP_s \tag{14}$$

where s is defined as the slip of the generator: $s = \dfrac{\omega_s - \omega_r}{\omega_s}$.

Therefore if the maximum slip is limited, say to 0.3, the rotor winding converters can be rated as a fraction of the induction generator rated power. This is typically around ±30% for DFIG in wind power generation systems gives a slip range of ±0.3. This is one key advantage of the DFIG system over fully-rated power electronic systems.

From the above relationships, the stator and rotor power are $P_s = P_m/(1–s)$ and $P_r = –sP_m/(1–s)$, respectively. To consider the mechanical power change during different rotor speeds, the following analysis is carried out with all terms in per unit values. The slip is assumed to vary from a sub-synchronous value of +0.35 to a super-synchronous valua of -0.35.

The per unit output power from wind turbine is

$$P_m = C_{p\_pu} V_{wind\_pu}^3 \tag{15}$$

Here we use the example wind turbine model in MATLAB (The Mathworks Inc., 2008): $C_p(\lambda,\beta) = c_1\left(\frac{c_2}{\lambda_i} - c_3\beta - c_4\right)e^{\frac{-c_5}{\lambda_i}} + c_6\lambda$, $\frac{1}{\lambda_i} = \frac{1}{\lambda + 0.08\beta} - \frac{0.035}{\beta^3 + 1}$, with the coefficients as c_1 = 0.5176, c_2 = 116, c_3 = 0.4, c_4 = 5, c_5 = 21 and c_6 = 0.0068. $\lambda = \frac{\omega_r R}{V_{wind}}$ is the tip-speed ratio.

The maximum value of C_p is 0.48 when β = 0 for λ = 8.1. These are defined as base values for per unit calculations. Here base wind speed is 12 m/s, gear ratio is 10, rotor radius is 5.16m. When s = –0.2, C_p is 0.48 then P_m is 1.0 p.u. ideally. Hence for 2 pole-pair generator, $s = \frac{\omega_s - \omega_r}{\omega_s}$, $\omega_{r\_pu} = 1 - s$, $\lambda = \frac{\omega_r R}{V_{wind}} = (1-s)\frac{5\pi \times 5.16}{12} = 6.751(1-s) = c_7(1-s)$.

Then at the base wind speed, the expression of P_m in terms of slip s is

$$P_m = \frac{C_p}{0.48} = \frac{1}{0.48}\left[c_1\left(\frac{c_2}{\lambda_i} - c_4\right)e^{\frac{-c_5}{\lambda_i}} + c_6 c_7(1-s)\right],\ \frac{1}{\lambda_i} = \frac{1}{c_7(1-s)} - 0.035\,. \tag{16}$$

The above analysis is carried out in MATLAB programming, with the power flow results shown in Fig. 9. Fig. 9 shows how the rotor and stator power vary as the rotor slip changes from sub- to super-synchronous modes. The speed of the rotor has to change as wind speed changes in order to track the maximum power point of the aerodynamic system. Slip, s, therefore is related to incident wind speed. In this case, a slip of -0.2 occurs with rated wind speed (12 ms^{-1}). As wind speed drops, slip has to increase and in this case has a maximum value of 0.35.

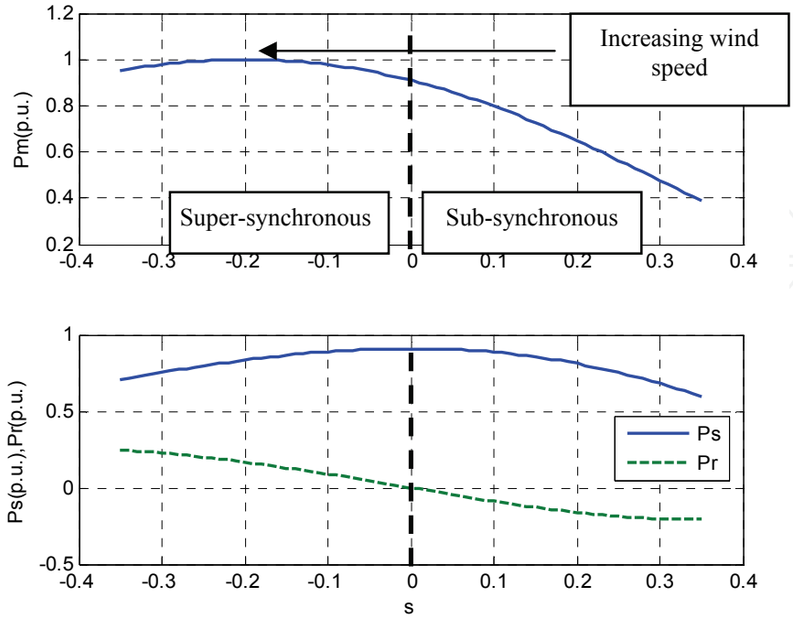

Fig. 9. Doubly-fed induction generation system power flows.

It is clear that the mechanical power, P_m, reaches its peak at super-synchronous speed when s = -0.2. When rotating at the synchronous speed (s = 0), the DFIG supplies all the power via the stator winding, with no active power flow in the rotor windings and their associated converters. Note that at s=0, the stator power is maximum. As the wind speed increases, the rotational speed must also increase to maintain optimum tip-speed ratios. In such circumstances, the machine operates at super-synchronous speeds (s < 0). The mechanical power flows to the grid through both the stator windings and the rotor windings and their converter. For example, at s=-0.2, P_s is 0.8pu and P_r is 0.2 pu giving a total generated power of 1pu. At lower wind speeds, the blades rotate at a sub-synchronous speed (s > 0). In such circumstances, the rotor converter system will absorb power from the grid connection to provide excitation for rotor winding. For example, at s=0.2, P_s is 0.8pu but P_r is -0.2 pu giving a total generated power of 0.6pu. With such a control scheme it is possible to control the power extracted from the aerodynamic system such that the blade operates at the optimum aerodynamic efficiency (thereby extracting as much energy is as possible) by adjusting the speed of rotation according to the incident wind speed.

The Rotor-Side Converter (RSC)

The rotor-side converter (RSC) applies the voltage to the rotor windings of the doubly-fed induction generator. The purpose of the rotor-side converter is to control the rotor currents such that the rotor flux position is optimally oriented with respect to the stator flux in order that the desired torque is developed at the shaft of the machine.

The rotor-side converter uses a torque controller to regulate the wind turbine output power and the voltage (or reactive power) measured at the machine stator terminals. The power is controlled in order to follow a pre-defined turbine power-speed characteristic to track the maximum power point. The actual electrical output power from the generator terminals, added to the total power losses (mechanical and electrical) is compared with the reference power obtained from the wind turbine characteristic. Usually, a Proportional-Integral (PI) regulator is used at the outer control loop to reduce the power error (or rotor speed error) to zero. The output of this regulator is the reference rotor current i_{rq}^{ref} that must be injected in the rotor winding by rotor-side converter. This q-axis component controls the electromagnetic torque T_e. The actual i_{rq} component of rotor current is compared with i_{rq}^{ref} and the error is reduced to zero by a current PI regulator at the inner control loop. The output of this current controller is the voltage v_{rq} generated by the rotor-side converter. With another similarly regulated i_{rd} and v_{rd} component the required 3-phase voltages applied to the rotor winding are obtained. The generic power control loop is illustrated in the next section.

The Grid-Side Converter (GSC)

The grid-side converter aims to regulate the voltage of the dc bus capacitor. Moreover, it is allowed to generate or absorb reactive power for voltage support requirements. The function is realized with two control loops as well: an outer regulation loop consisting of a dc voltage regulator. The output of the dc voltage regulator is the reference current i_{cd}^{ref} for the current regulator. The inner current regulation loop consists of a current regulator controlling the magnitude and phase of the voltage generated by converter from the i_{cd}^{ref} produced by the dc voltage regulator and specified q-axis i_{cq}^{ref} reference.

Converter losses

The losses of the converters can be divided into switching losses and conducting losses. The switching losses of the transistors are the turn-on and turn-off losses. For the diode the

switching losses mainly consist of turn-off losses, i.e., reverse-recovery energy. The turn-on and turn-off losses for the transistor and the reverse-recovery energy loss for a diode can be found from data sheets. The conducting losses arise from the current through the transistors and diodes. The transistor and the diode can be modeled as constant voltage drops, and a resistance in series. The switching losses of the transistor can be considered to be proportional to the current, for a given dc-link voltage. For a given dc-link voltage and switching frequency, the switching losses of the IGBT and diode can be modeled as a constant voltage drop that is independent of the current rating of the valves (Petersson, 2005).

DC-link model

The dc-link model describes the dc-link capacitor voltage variations as a function of the input power to the dc-link (Ledesma & Usaola, 2005). The energy stored in the dc capacitor is

$$W_{dc} = \int P_{dc} dt = \frac{1}{2} C V_{dc}^2 \tag{17}$$

Where C is the capacitance, V_{dc} is the voltage, W_{dc} is the stored energy, and P_{dc} is the input power to the dc link. The voltage and energy derivatives are

$$\frac{dV_{dc}}{dt} = \frac{P_{dc}}{CV_{dc}}, \quad \frac{dW_{dc}}{dt} = P_{dc} \tag{18}$$

The P_{dc} is calculated as $P_{dc} = P_{in} - P_c$. Where P_{in} is the input power from rotor-side converter and P_c is the grid-side converter output power. The dc-link voltage varies as P_{dc} and is a constant when $P_{dc} = 0$.

Basic Control of Real and Reactive Power using the RSC

The grid side converter is used to partly control the flow of real and reactive power from the turbine system to the grid. The grid-side converter feeds the grid via a set of interfacing inductors. Figure 9(a) shows the single phase equivalent circuit of the system. As previously shown, the grid-side converter (a voltage source inverter) can generate a balanced set of three-phase voltages at the supply frequency and that the voltage, E, can have a controllable magnitude and phase. Load angle control is used to illustrate the basics of real and reactive power control, though in practise, a more sophisticated control is used which provides superior transient response. Load angle control mimics the operation of a synchronous generator connected to the network. Essentially, load angle control uses the angle, δ, between the voltage generated by the grid-side converter, E, and the grid voltage, V, Figure 11(b), to control the real power, P, injected on to the grid. Likewise, reactive power, Q, is controlled using the magnitude of the voltage generated by the grid-side converter. The steady-state equations governing the real and reactive power flow from the grid-side converter to the grid are

$$P = \frac{VE\sin\delta}{X_s} \quad and \quad Q = \frac{V^2}{X_s} - \frac{VE}{X_s}\cos\delta \tag{19}$$

where X_s is the reactance of the interfacing inductance. If δ is small the equations can be simplified to

$$P = \frac{VE\delta}{X_s} \quad and \quad Q = \frac{V^2}{X_s} - \frac{VE}{X_s} \tag{20}$$

Showing that P can be controlled using load angle, δ, and Q can be controlled using the magnitude of E. Interfacing inductance must be used to couple the output of the grid-side converter shown in Figure 8 to the grid. The inductor is sized according to the rating of the converter. Typically, the system will have a transformer on the turbine side of the point of common coupling (PCC). In addition, at the point of connection there is usually the need for a substation which includes whatever equipment is required by local network codes, for example, plant to disconnect the turbine under fault conditions.

The combination of control and power electronics enables the grid-side converter to produce the necessary voltage magnitude, E, and load angle, δ, in order to meet a required P_c and Q_c demand set by the main system controller. The controller has to be able to synchronise to the grid frequency and phase, in order to connect and supply power. This is typically carried out using some form of phase-locked loop.

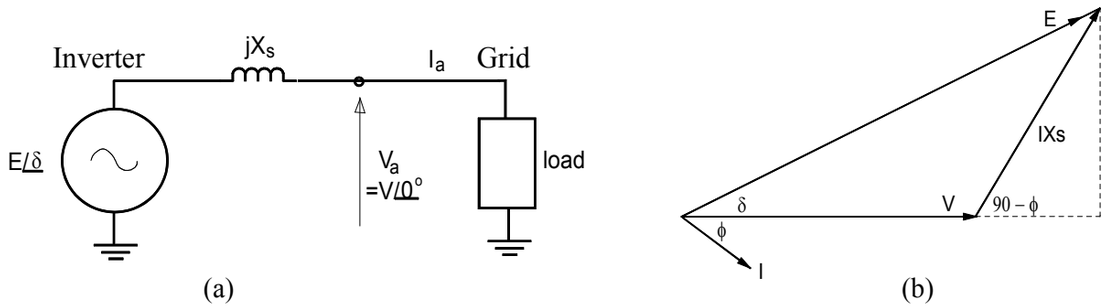

Fig. 10. (a) Single line diagram of steady-state generator-side converter connected to the grid and (b) phasor diagram demonstrating load angle control of the grid-side converter to establish exported real power and control of reactive power

At any instant, the power exported by the GSC is determined by the state of the DC link voltage. The grid-side converter controller monitors the DC link voltage. If the DC link voltage rises, the grid-side converter can export more real power by increasing the load angle in order that the DC link voltage moves back towards it nominal value. If more power is being exported by the GSC than is currently being generated by the RSC, the DC link voltage will fall below its nominal value. The grid-side controller will then reduce the exported real power to allow the DC link voltage to recover to its nominal value. In essence the DC link voltage indicates power flow balance between the generated energy and the exported energy in the rotor side. If the input and output power to the dc link capacitor do not match then the dc link voltage will change.

The quality of the energy supplied to the network must meet basic requirements and these will be set by the 'Grid Code' in force at the connection point. The grid code specifies many performance indicators of the quality of the energy supplied by the grid-side converter, along with other important issues such as fault levels, anti-islanding and disconnection. The relevant grid code(s) in operation must be determined prior to tendering for work on the turbine power electronics and control.

The grid code has important implications on the control system of the turbine. One main concern in many turbine systems is what to do if the turbine system loses its mains

connection, say, for example, because of a network fault. Without a mains connection the turbine is unable to export energy. If the generator-side controller continues to generate power, the DC link capacitance will be over charged. Therefore, a grid fault will require the generator to stop generating energy, which then means that there is no longer a restraining torque to control the blade speed. In a wind turbine, a loss of supply will cause an over-speed condition, as the blade system will accelerate due to the aerodynamic torque produced by the blades. Shorting resistors, or a crowbar circuit, are often switched across the rotor circuit of the generator in order that the energy generated by the blade system can be absorbed and the over-speed condition controlled to a safe and manageable level. In addition, there are often aerodynamic (pitch control) and mechanical braking mechanisms included in wind turbines as an additional over-speed safety measure.

4. Control system

Nomenclature

$\vec{v}$, $\vec{i}$, $\vec{\psi}$	Voltage, current and flux vectors.
R_s, R_r	Stator, rotor winding resistances.
L_s, L_r, L_{ls}, L_{lr}	Stator, rotor winding self- and leakage inductances.
L_m	Magnetizing inductance.
ω_s, ω_r, ω_{slip}	Synchronous, rotor and slip angular frequencies.
P, Q	Active and reactive power.
s, r	Stator and rotor subscripts.
g	Grid-side value subscripts.
c	Converter value subscripts.
d, q	d-axis and q-axis component subscripts.
n	Nominal value subscript.
ref	Reference value superscript.

This section will detail the vector-control techniques used for the independent control of torque and rotor excitation current in the DFIG and decouple control of the active and reactive power supplied to the grid. The vector control for the generator can be embedded in an optimal power tracking controller for maximum energy capture in a wind power application. By controlling the active power of the converter, it is possible to vary the rotational speed of the generator, and thus the speed of the rotor of the wind turbine. This can then be used to track the optimum tip-speed ratio as the incident wind speed changes thereby extracting the maximum power from the incident wind. The grid-side converter control gives potential for optimising the grid integration with respect to steady-state operation conditions, power quality and voltage stability.

4.1 Rotor-side converter control

The rotor-side converter (RSC) provides the excitation for the induction machine rotor. With this PWM converter it is possible to control the torque hence the speed of the DFIG and also the power factor at the stator terminals. The rotor-side converter provides a varying excitation frequency depending on the wind speed conditions. The induction machine is controlled in a synchronously rotating dq-axis frame, with the d-axis oriented along the stator-flux vector position in one common implementation. This is called stator-flux orientation (SFO) vector control. In this way, a decoupled control between the electrical

torque and the rotor excitation current is obtained. Consequently, the active power and reactive power are controlled independently from each other.

There are other options for directional rotating frames. Orientation frames applied in traditional vector control of induction machines such as rotor-flux orientation and magnetizing-flux orientation, can also be utilised (Vas, 1990). Additionally, the stator-voltage orientation (SVO) is also commonly-used in DFIG vector controller, as contrast with SFO (Muller et al., 2002).

To describe the control scheme, the general Park's model of an induction machine is introduced. Using the motor convention in a static stator-oriented reference frame, without saturation, the voltage vector equations are

$$\vec{v}_s = R_s \vec{i}_s + \frac{d\vec{\psi}_s}{dt} \tag{21}$$

$$\vec{v}_r = R_r \vec{i}_r + \frac{d\vec{\psi}_r}{dt} - j\omega\vec{\psi}_r \tag{22}$$

where $\vec{v}_s$ is the stator voltage imposed by the grid. The rotor voltage $\vec{v}_r$ is controlled by the rotor-side converter and used to perform generator control.

The flux vector equations are

$$\vec{\psi}_s = L_s \vec{i}_s + L_m \vec{i}_r \tag{23}$$

$$\vec{\psi}_r = L_m \vec{i}_s + L_r \vec{i}_r \tag{24}$$

where L_s and L_r are the stator and rotor self-inductances: $L_s = L_m + L_{ls}$, $L_r = L_m + L_{lr}$.

Under stator-flux orientation (SFO), in *dq*-axis component form, the stator flux equations are:

$$\begin{cases} \psi_{sd} = L_s i_{sd} + L_m i_{rd} = \psi_s = L_m i_{ms} \\ \psi_{sq} = 0 \end{cases} \tag{25}$$

Defining leakage factor $\sigma = 1 - \frac{L_m^2}{L_s L_r}$ and equivalent inductance as $L_o = \frac{L_m^2}{L_s}$. The rotor voltage and flux equations are (scaled to be numerically equal to the ac per-phase values):

$$\begin{cases} v_{rd} = R_r i_{rd} + \sigma L_r \frac{di_{rd}}{dt} - \omega_{slip}\sigma L_r i_{rq} \\ v_{rq} = R_r i_{rq} + \sigma L_r \frac{di_{rq}}{dt} + \omega_{slip}(L_o i_{ms} + \sigma L_r i_{rd}) \end{cases} \tag{26}$$

$$\begin{cases} \psi_{rd} = \frac{L_m^2}{L_s} i_{ms} + \sigma L_r i_{rd} \\ \psi_{rq} = \sigma L_r i_{rq} \end{cases} \tag{27}$$

where the slip angular speed is $\omega_{slip} = \omega_s - \omega_r$.

The stator flux angle is calculated from

$$\begin{cases} \psi_{s\alpha} = \int (v_{s\alpha} - R_s i_{s\alpha}) dt \\ \psi_{s\beta} = \int (v_{s\beta} - R_s i_{s\beta}) dt \end{cases}, \quad \theta_s = \tan^{-1}\left(\frac{\psi_{s\beta}}{\psi_{s\alpha}}\right) \tag{28}$$

where θ_s is the stator-flux vector position.

The control scheme of the rotor-side converter is organised in a generic way with two series of two PI-controllers. Fig. 11 shows a schematic block diagram for the rotor-side converter control. The reference q-axis rotor current i_{rq}^* can be obtained either from an outer speed-control loop or from a reference torque imposed on the machine. These two options may be termed a speed-control mode or torque-control mode for the generator, instead of regulating the active power directly. For speed-control mode, one outer PI controller is to control the speed error signal in terms of maximum power point tracking. Furthermore, another PI controller is added to produce the reference signal of the d-axis rotor current component to control the reactive power required from the generator. Assuming that all reactive power to the machine is supplied by the stator, the reference value i_{rd}^* may set to zero. The switching dynamics of the IGBT-switches of the rotor converter are neglected and it is assumed that the rotor converter is able to follow demand values at any time.

The control system requires the measurement of the stator and rotor currents, stator voltage and the mechanical rotor position. There is no need to know the rotor-induced EMF, as is the case for the implementation with naturally commutated converters. Since the stator is connected to the grid, and the influence of the stator resistance is small, the stator magnetising current i_{ms} can be considered constant (Pena et al., 1996).

Rotor excitation current control is realised by controlling rotor voltage. The i_{rd} and i_{rq} error signals are processed by associated PI controllers to give v_{rd} and v_{rq}, respectively.

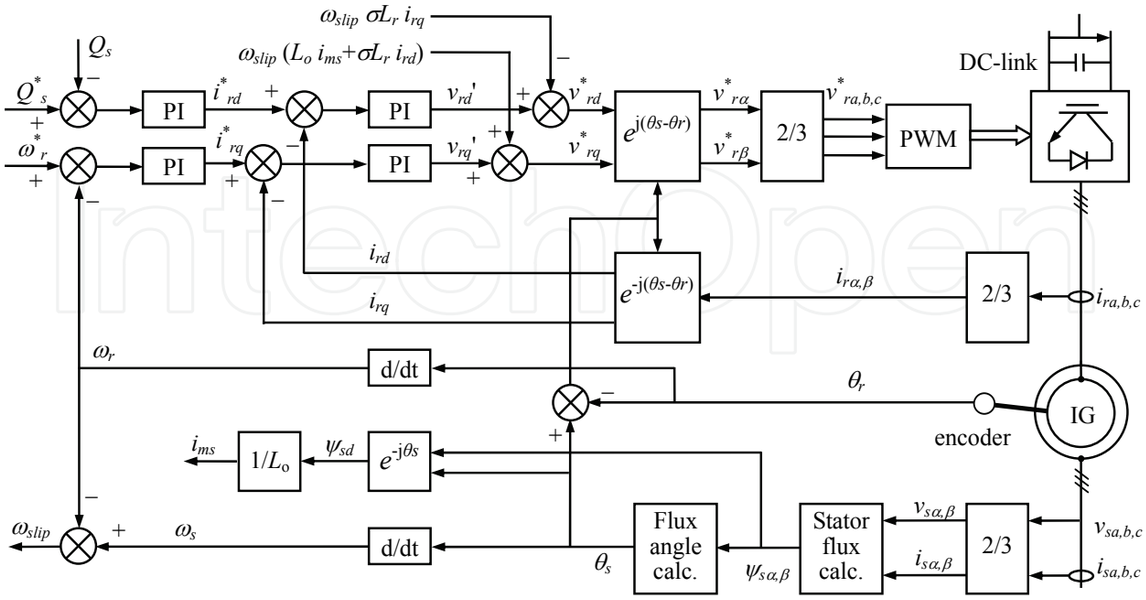

Fig. 11. Vector control structure for rotor-side converter.

From the rotor voltage equations (26) define

$$\begin{cases} v'_{rd} = R_r i_{rd} + \sigma L_r \dfrac{di_{rd}}{dt} \\ v'_{rq} = R_r i_{rq} + \sigma L_r \dfrac{di_{rq}}{dt} \end{cases} \tag{29}$$

To ensure good tracking of the rotor dq-axis currents, compensation terms are added to v'_{rd} and v'_{rq} to obtain the reference voltages v_{rd}^* and v_{rq}^* according to

$$\begin{cases} v_{rd}^* = v'_{rd} - \omega_{slip}\sigma L_r i_{rq} \\ v_{rq}^* = v'_{rq} + \omega_{slip}(L_m i_{ms} + \sigma L_r i_{rd}) \end{cases} \tag{30}$$

The electromagnetic torque is

$$T_e = -\frac{3}{2} p \,\mathrm{Im}\left\{ \vec{\psi}_s \vec{i}_r^* \right\} = -\frac{3}{2} p L_o i_{ms} i_{rq} \,. \tag{31}$$

For the stator-voltage oriented control the above equation is an approximation. However, for stator-flux orientation, the stator flux current i_{ms} is almost fixed to the stator voltage. For torque mode control, since it is difficult to measure the torque, it is often realised in an open-loop manner. The torque can be controlled by the q-axis component of the rotor current i_{rq}. Therefore, the q-axis reference current, i_{rq}^{ref} can be determined from the reference torque T_e^{ref} as

$$i_{rq}^{ref} = -\frac{2T_e^{ref}}{3pL_o i_{ms}} = -\frac{2T_e^{ref}}{3p\psi_s} \tag{32}$$

4.2 Grid-side converter control

The grid-side converter controls the flow of real and reactive power to the grid, through the grid interfacing inductance. The objective of the grid-side converter is to keep the dc-link voltage constant regardless of the magnitude and direction of the rotor power. The vector-control method is used as well, with a reference frame oriented along the stator voltage vector position, enabling independent control of the active and reactive power flowing between the grid and the converter. The PWM converter is current regulated, with the d-axis current used to regulate the dc-link voltage and the q-axis current component to regulate the reactive power. Fig. 12 shows the schematic control structure of the grid-side converter.

A similar analysis for the control of the dq currents carried out for the grid-side converter can likewise be done for the control of the converter dq currents. The voltage equations in synchronously rotating dq-axis reference frame are:

$$\begin{cases} v_{cd} = Ri_{cd} + L_{choke}\dfrac{di_{cd}}{dt} - \omega_e L_{choke} i_{cq} + v_{cd1} \\ v_{cq} = Ri_{cq} + L_{choke}\dfrac{di_{cq}}{dt} + \omega_e L_{choke} i_{cd} + v_{cq1} \end{cases} \tag{33}$$

The angular position of the grid voltage is calculated as $\theta_e = \int \omega_e dt = \tan^{-1}\left(\frac{v_{c\beta}}{v_{c\alpha}}\right)$

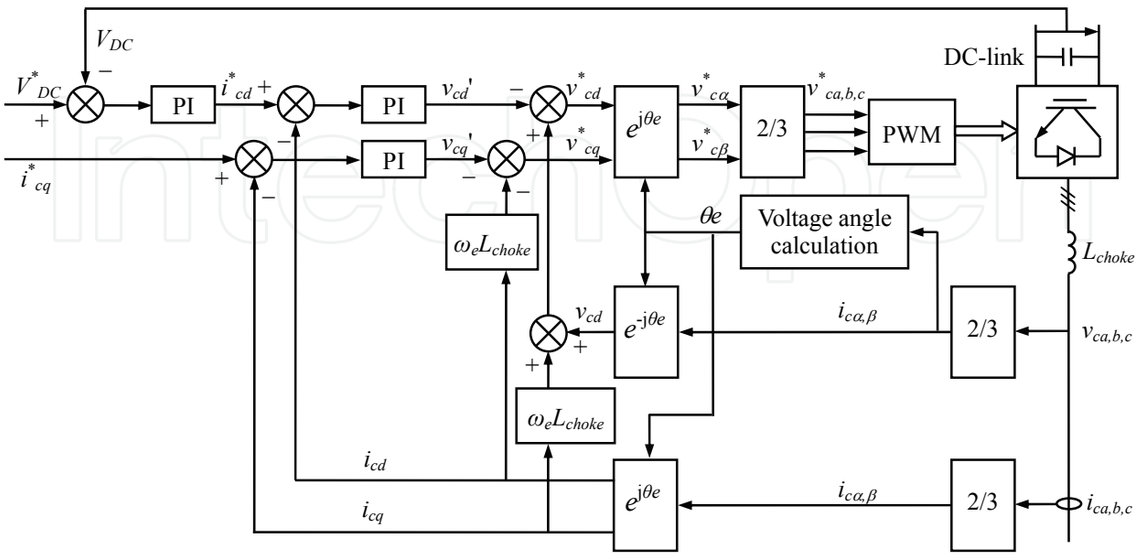

Fig. 12. Vector control structure for grid-side converter.

where $v_{c\alpha}$ and $v_{c\beta}$ are the converter grid-side voltage stationary frame components.
The *d*-axis of the reference frame is aligned with the grid voltage angular position θ_e. Since the amplitude of the grid voltage is constant, v_{cq} is zero and v_{cd} is constant. The active and reactive power will be proportional to i_{cd} and i_{cq} respectively.
Assume the grid-side transformer connection is star, the converter active and reactive power flow is

$$\begin{cases} P_c = 3(v_{cd}i_{cd} + v_{cq}i_{cq}) = 3v_{cd}i_{cd} \\ Q_c = 3(v_{cd}i_{cq} + v_{cq}i_{cd}) = 3v_{cd}i_{cq} \end{cases} \tag{34}$$

Which demonstrates that the real and active powers from the grid-side converter are controlled by the i_{cd} and i_{cq} components of current respectively. To realise decoupled control, similar compensations are introduced likewise in equation (30):

$$\begin{cases} v^*_{cd} = -v'_{cd} + (\omega_e L_{choke} i_{cq} + v_d) \\ v^*_{cq} = -v'_{cq} - (\omega_e L_{choke} i_{cd}) \end{cases} \tag{35}$$

The reference voltage v_{cd}^* and v_{cq}^* are then transformed by inverse-Park transformation to give 3-phase voltage v_{cabc}^* for the final PWM signal generation for the converter IGBT switching.

5. Application issues

5.1 Industrial applications

The DFIG system costs more than fixed-speed induction generators without converters. However, the performance and controllability are excellent in comparison with fixed-

speed induction generator systems; they capture more wind energy, they exhibit a higher reliability gear system, and high-quality power supplied to the grid. It saves investment on full-rated power converters, and soft-starter or reactive power compensation devices (fixed-speed systems). Modern wind farms, with a nominal turbine power up to several MWs, are a typical case of DFIG application. Besides this, other applications for the DFIG systems are, for example, flywheel energy storage system, stand-along diesel systems, pumped storage power plants, or rotating converters feeding a railway grid from a constant frequency utility grid.

5.2 Braking systems

Braking systems for a wind turbine generation system must be able to reduce the speed of the aerodynamic rotor during abnormal scenarios, such as over speed, maintenance or fault conditions. Wind turbine design standards require two independent brakes which must be capable of reducing the wind turbine to a safe rotational speed in all anticipated wind speeds and fault conditions (Craig et al., 1998). There are usually combined conventional mechanical shaft (disk) brakes and aerodynamic brakes (for example, pitching mechanisms) for wind turbine brake systems. For a rapid response, electrodynamic braking can be used but only in the event that the electrical systems are operational. However, it has to be used in combination with a mechanical parking brake in cases when the rotor cannot be allowed to idle at a low rotational speed. Moreover, it cannot hold the rotor at standstill.

5.3 Converter protection systems

The prevalent DFIG converter protection scheme is crowbar protection. A crowbar is a set of resistors that are connected in parallel with the rotor winding on occurrence of an interruption. The crowbar circuit bypasses the rotor-side converter. The active crowbar control scheme connects the crowbar resistance when necessary and disables it to resume DFIG control. A braking resistor (DC-chopper) can be connected in parallel with the DC-link capacitor to limit the overcharge during low grid voltage. This protects the IGBTs from overvoltage and can dissipate energy, but this has no effect on the rotor current. It is also used as protection for the DC-link capacitor in full rated converter topologies, for example, permanent magnet synchronous generators. In a similar way to the series dynamic braking resistor, which has been used in the stator side of generators, a dynamic resistor is proposed to be put in series with the rotor (series dynamic resistor) and this limits the rotor over-current (Yang et al., 2010). Being controlled by a power-electronic switch, in normal operation, the switch is on and the resistor is bypassed; during fault conditions, the switch is off and the resistor is connected in series to the rotor winding. The rotor equivalent circuit is shown with all the above protection schemes in Fig. 13.

6. Summary

The DFIG system applied to wind power generation has gained considerable academic attention and industrial application during the past 10 years. In practical applications, power levels are currently reaching 3-5MW and the DFIG is gradually maturing as a

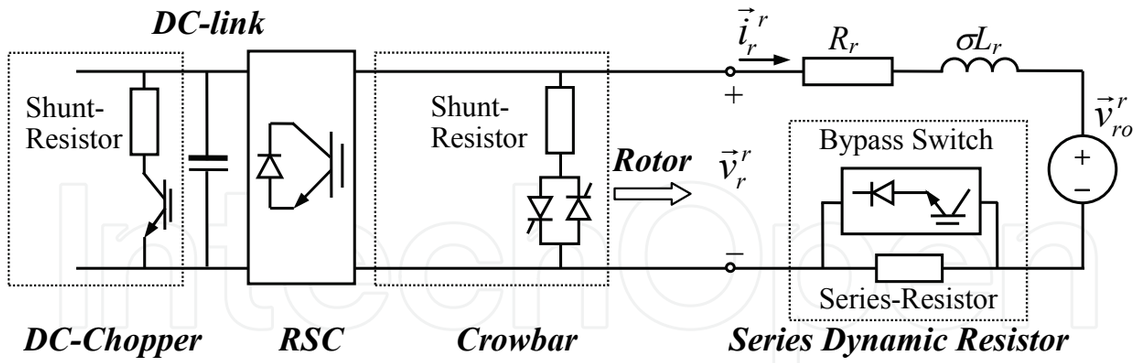

Fig. 13. DFIG rotor equivalent circuit with all protection schemes shown.

technology for variable-speed wind energy utilisation. In this chapter, the steady-state induction machine operation, back-to-back converter system and basic vector-control techniques are summarised, with practical application issues briefly summarised. Although topologies of new systems with improved performance are emerging both in academia and industry (Chen et al., 2009), DFIG is the most competitive option in terms of balance between the technical performance and economic costs.

7. References

Chen, Z.; Guerrero, J.M. & Blaabjerg, F. (2009). A review of the state of the art of power electronics for wind turbines, *IEEE Trans. Power Electron.,* Vol. 24, No. 8, August 2009, 1859-1875, ISSN 0885-8993

Craig, L.M.; Saad-Saoud, Z. & Jenkins, N. (1998). Electrodynamic braking of wind turbines, *IEE Proc.-Electr. Power Appl.,* Vol. 145, No. 2, March 1998, 140-146, ISSN

Ledesma, P. & Usaola, J. (2005). Doubly fed induction generator model for transient stability analysis, *IEEE Trans. Energy Conver.,* Vol. 20, No. 2, June 2005, 388-397, ISSN 0885-8969

Muller, S.; Deicke, M. & De Doncker, R.W. (2002). Doubly fed induction generator systems for wind turbines, *IEEE Ind. Appl. Magazine,* Vol., No., May/June 2002, 26-33, ISSN 1077-2618/02

Pena, R.; Clare, J.C. & Asher, G.M. (1996). Doubly fed induction generator using back-to-back PWM converters and its application to variable-speed wind-energy generation, *IEE Proc.-Electr. Power Appl.,* Vol. 143, No. 3, May 1996, 231-241, ISSN

Petersson, A. (2005). *Analysis, modeling and control of doubly-fed induction generators for wind turbines,* Chalmers University of Technology, Goteborg, Sweden, 2005.

The Mathworks Inc. (2008). MATLAB (R2008a), Product Help.

Vas, P. (1990). *Vector Control of AC Machines,* Oxford University Press, ISBN 0 19 859370 8, Oxford, UK.

Yang, J.; Fletcher, J.E. & O'Reilly, J. (2010). A Series-dynamic-resistor-based converter protection scheme for doubly-fed induction generator during various fault conditions, *IEEE Trans. Energy Conver.,* Vol. 25, No. 2, June 2010, 422-432, ISSN 0885-8969

Paths to Sustainable Energy
Edited by Dr Artie Ng

ISBN 978-953-307-401-6
Hard cover, 664 pages
Publisher InTech
Published online 30, November, 2010
Published in print edition November, 2010

The world's reliance on existing sources of energy and their associated detrimental impacts on the environment- whether related to poor air or water quality or scarcity, impacts on sensitive ecosystems and forests and land use - have been well documented and articulated over the last three decades. What is needed by the world is a set of credible energy solutions that would lead us to a balance between economic growth and a sustainable environment. This book provides an open platform to establish and share knowledge developed by scholars, scientists and engineers from all over the world about various viable paths to a future of sustainable energy. It has collected a number of intellectually stimulating articles that address issues ranging from public policy formulation to technological innovations for enhancing the development of sustainable energy systems. It will appeal to stakeholders seeking guidance to pursue the paths to sustainable energy.

INTECH
open science | open minds

InTech Europe
University Campus STeP Ri
Slavka Krautzeka 83/A
51000 Rijeka, Croatia
Phone: +385 (51) 770 447
Fax: +385 (51) 686 166
www.intechopen.com

InTech China
Unit 405, Office Block, Hotel Equatorial Shanghai
No.65, Yan An Road (West), Shanghai, 200040, China
中国上海市延安西路65号上海国际贵都大饭店办公楼405单元
Phone: +86-21-62489820
Fax: +86-21-62489821

IntechOpen